

REPORT DOCUMENTATION PAGE			Form Approved OMB NO. 0704-0188	
Public Reporting burden for this collection of information is estimated to average 1 hour per response, including the time for reviewing instructions, searching existing data sources, gathering and maintaining the data needed, and completing and reviewing the collection of information. Send comment regarding this burden estimates or any other aspect of this collection of information, including suggestions for reducing this burden, to Washington Headquarters Services, Directorate for information Operations and Reports, 1215 Jefferson Davis Highway, Suite 1204, Arlington, VA 22202-4302, and to the Office of Management and Budget, Paperwork Reduction Project (0704-0188,) Washington, DC 20503.				
1. AGENCY USE ONLY (Leave Blank)		2. REPORT DATE		3. REPORT TYPE AND DATES COVERED
4. TITLE AND SUBTITLE			5. FUNDING NUMBERS	
6. AUTHOR(S)				
7. PERFORMING ORGANIZATION NAME(S) AND ADDRESS(ES)			8. PERFORMING ORGANIZATION REPORT NUMBER	
9. SPONSORING / MONITORING AGENCY NAME(S) AND ADDRESS(ES) U. S. Army Research Office P.O. Box 12211 Research Triangle Park, NC 27709-2211			10. SPONSORING / MONITORING AGENCY REPORT NUMBER	
11. SUPPLEMENTARY NOTES The views, opinions and/or findings contained in this report are those of the author(s) and should not be construed as an official Department of the Army position, policy or decision, unless so designated by other documentation.				
12 a. DISTRIBUTION / AVAILABILITY STATEMENT Approved for public release; distribution unlimited.			12 b. DISTRIBUTION CODE	
13. ABSTRACT (Maximum 200 words)				
14. SUBJECT TERMS			15. NUMBER OF PAGES	
			16. PRICE CODE	
17. SECURITY CLASSIFICATION OR REPORT UNCLASSIFIED	18. SECURITY CLASSIFICATION ON THIS PAGE UNCLASSIFIED	19. SECURITY CLASSIFICATION OF ABSTRACT UNCLASSIFIED	20. LIMITATION OF ABSTRACT UL	

NSN 7540-01-280-5500

Standard Form 298 (Rev.2-89)
Prescribed by ANSI Std. Z39-18
298-102

Enclosure 1

Foreword

The goal of this program is to develop avalanche photodiodes (APDs) and APD arrays for applications in the mid-infrared (MIR). Detectors that operate in this wavelength range require high sensitivity to enhance the performance of applications such as night vision, infrared spectroscopy, gas sensing, target identification and detection, and remote sensing. Our results to date include:

- Demonstration of photodiodes (PIN photodiodes and APDs) operating at 2.4 μm
- Initial design of absorption regions which will cover the entire MIR
- Initial experimental results on strained strain-compensated absorption regions with expected absorption out to 4.5 μm .

Statement of the problem studied

The main objective of this research program is to extend avalanche photodiodes (APDs) – which are a mainstream technology for fiber optic communications – into the MIR. APDs make an outstanding technology for this wavelength regime for two main reasons. First, APDs use multiplication regions to enhance the signal-to-noise ratio of incoming photons. Second, the noise characteristics can be minimized by careful design of the multiplication region, an area in which the principal investigator has been involved previously[1-10]. Low noise also increases the sensitivity of the detector.

The approach we have pursued for MIR detection on InP is a superlattice consisting of $\text{Ga}_x\text{In}_{1-x}\text{As}$ and $\text{GaAs}_y\text{Sb}_{1-y}$ alloys. Optical transitions for this heterostructure are type-II. This means that electrons from the valence band of GaAsSb move to the conduction band of GaInAs when a photon is absorbed. These electrons and holes are then collected at the contacts as current. **Thus, the detection wavelength is not a direct function of the band gaps of GaInAs and GaAsSb.** This provides two advantages for MIR detection. First, a large (greater than 700 meV) direct band-gap for both GaInAs and GaAsSb should lead to a lower thermal carrier generation rate than a material with a smaller direct band gap, resulting in a significant reduction in dark current. Second, the variation of layer thickness and the addition of strain compensation between the two layers can be used to create longer wavelength detection since these design variables affect the formation of mini-bands in the superlattice. This flexibility in customizing the detection wavelength is a tremendous benefit of the superlattice approach.

The success of this project will have substantial impact on both commercial and military applications. On the commercial side, these applications include high resolution molecular spectroscopy, trace gas monitoring, air pollution analysis, remote sensing, and non-invasive medical diagnostics. On the military side, applications include night vision, target identification and detection, infrared thermal sensors, and laser radar (LADAR).

Summary of Important results

Initial Demonstration of APDs using GaAsSb/GaInAs superlattices

To demonstrate that these superlattices can be used in photodiodes, we have designed, fabricated, and tested an InP-based APD with a cutoff wavelength of 2.4 μm . The absorption region of this photodiode contained a 150-period superlattice of lattice-matched GaInAs and GaAsSb (compositions are $\text{Ga}_{0.47}\text{In}_{0.53}\text{As}$ and $\text{GaAs}_{0.51}\text{Sb}_{0.49}$ respectively) Each layer had a thickness of 5 nm leading to a total absorption region thickness of 1.5 μm . In this device, a separate absorption, charge, and multiplication (SACM) structure was used to keep the electric field low in the absorption region. InP was used for the multiplication region and the structure was designed to have holes injected into the multiplication regions to initiate the multiplication process. The device structure is shown in Figure 1 below.

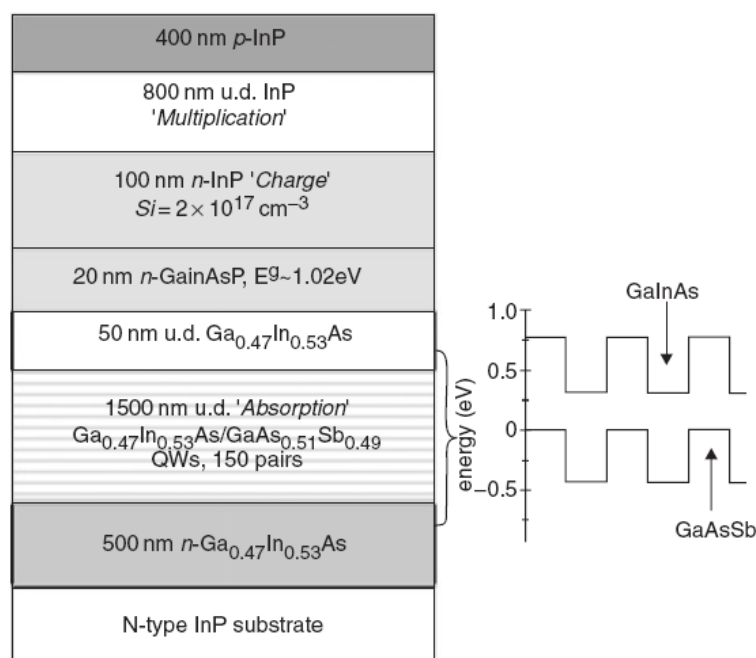


Figure 1: Device schematic for a MIR SACM APD.

Mesa devices of different diameters were fabricated using standard photolithography and wet etching techniques. An etch chemistry of $\text{H}_3\text{PO}_4:\text{H}_2\text{O}_2:\text{H}_2\text{O}$ (1:1:10) was used for both GaInAs and GaAsSb. SiO_2 was used to passivate the mesa walls to minimize edge leakage currents. Ti/Pt/Au and AuGe/Ni/Au were deposited for p- and n-metal contacts. Electroplated Au air-bridges were used to connect the p-metal from the mesa tops to the p-pads. N-pads were deposited directly on the n-metal contacts. Devices were contacted by wire-bonding to the p- and n- pads. The current-voltage characteristics for the APD is shown in Figure 2.

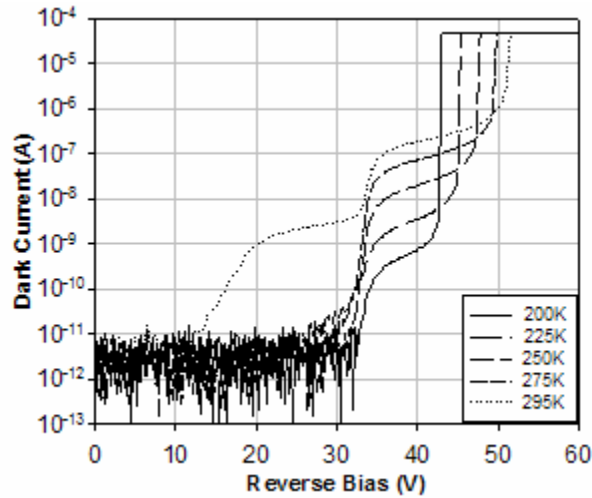


Figure 2: Dark current vs. reverse bias voltage from a 44 μm -diameter device, measured at 200K, 225K, 250K, 275K, and 295K

Room temperature dark current at punchthrough (-37V) is 130nA for a 44 μm -diameter device. The dark current drops rapidly with temperature, and at 225K, the dark current at 90% of breakdown is approximately 10nA, corresponding to current density of 0.66 mA/cm². This reduction in dark current shows the advantage of the SACM structure.

The gain at punchthrough was determined by comparing the photocurrent from a 64 μm diameter APD biased at -37V to the photocurrent of a p-i-n device of the same size, under the same illumination from a 1.55 μm wavelength laser. The ratio of the photocurrents at room temperature was 1.7, which was assumed to be the gain of the APD at -37V. The gain curves as a function of bias voltage are plotted in Figure 3.

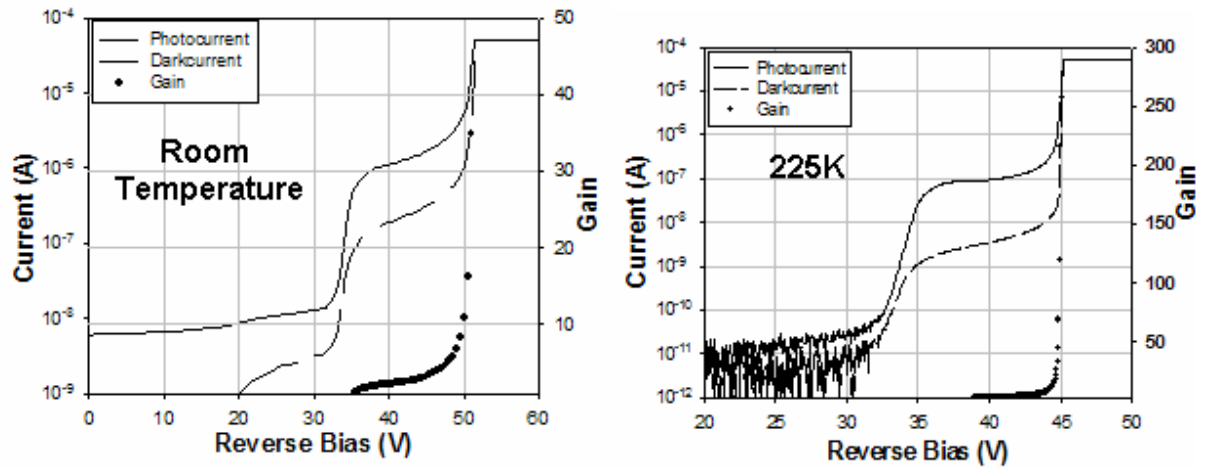


Figure 3: Reverse I-V and gain at room temperature and 225K

As can be seen in Figure 3, we have observed gains in excess of 20 at room temperature and in excess of 100 at 225K. As long as the noise current does not increase significantly at these biases, the D^* value will increase with multiplication gain. Our initial work suggests that this is the case and more work is ongoing to quantify the improvement in D^* for APDs.

Design of MIR Absorption Regions

In the initial device results, lattice-matched GaInAs and GaAsSb was used in the absorption region. Given the fixed compositions for lattice-matched materials, the detection wavelength is also fixed. Thus, extending the wavelength further into the MIR will require strain be added to the materials. Using Model Solid Theory[1], we have done an initial investigation of the strains needed. The results are shown in Figure 4 below.

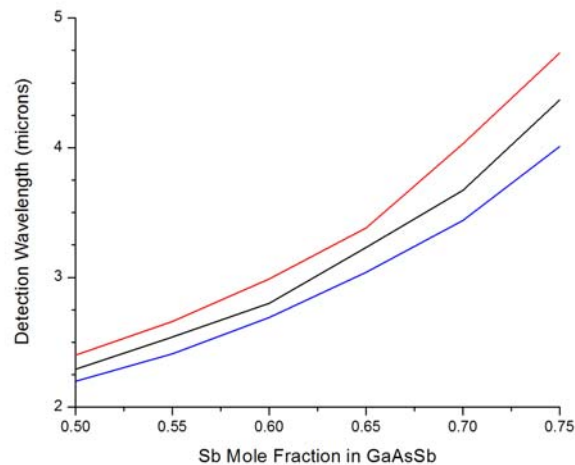


Figure 4: Calculated Emission wavelength from a GaAsSb/GaInAs superlattice at room temperature. The thickness of the GaAsSb layers are 3 nm and the thickness of the GaInAs layers are 5 nm. The color sequence is compressively strained GaInAs (red), lattice matched GaInAs (black), and tensile strained GaInAs (blue).

For the absorption regions of photodiodes, strain compensation must be used. The results above show that wavelengths near 4 μm are easily obtainable. Increased strain will be needed to push the detection wavelength out to 5 μm .

Experimental Work on Strain Compensated MIR Absorption Regions

We have begun work to show that the predictions for Figure 4 are valid. The first experiment was looking at the effects of compressive strain in GaAsSb on the detection wavelength. Based upon our predictions, the wavelength should extend further into the MIR. Figure 5 shows the initial results. The peak wavelengths vary from 3.2 μm to 3.8 μm as the amount of Sb used is increased. The longest wavelength sample (Sb:As ratio of 3:1) has optical response beyond 4.5 μm . This shows that GaAsSb/GaInAs superlattices are a viable candidate for MIR detectors.

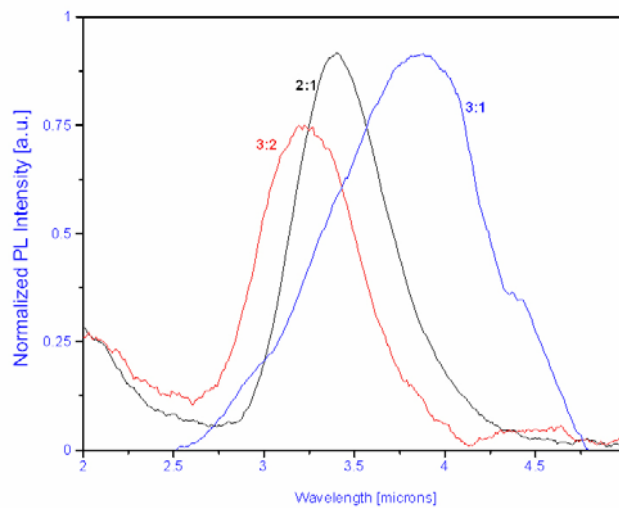


Figure 5: Normalized Photoluminescence for strained GaAsSb/GaInAs superlattices with Sb:As ratios of 3:2 (red), 2:1 (black), and 3:1 (blue). The data shown has been smoothed to remove the noise from the measurement.

In work with Luke Mawst at Wisconsin, we have begun to look at the growth of strain compensation of these superlattices. Figure 6 shows the initial structures. Our modeling predicted wavelengths in excess of 3.5 μm in these structures.

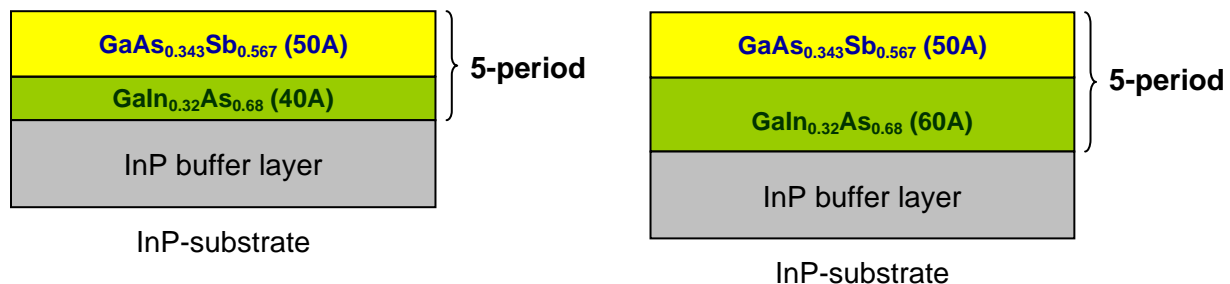


Figure 6: Initial structures for strain-compensated GaAsSb/GaInAs superlattices for MIR absorption regions.

The x-ray diffraction results are shown in Figure 7.

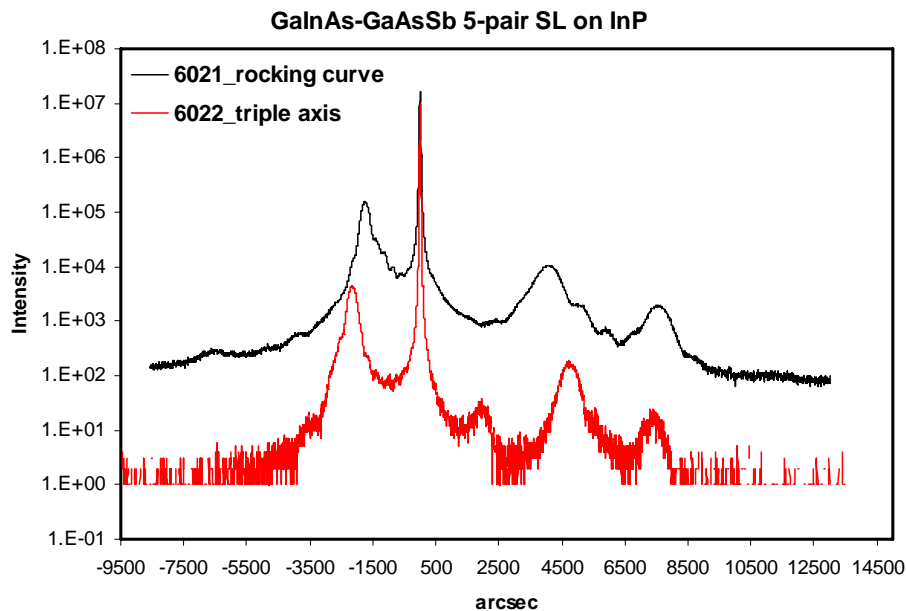


Figure 7: XRD of the initial strain compensation structure. 6021 refers to the structure on the left of Figure 6; 6022 refers to the structure on the right.

We see evidence of partial strain relaxation in these structures due to the broadness of the superlattice peaks. We are working on measuring the room-temperature PL from these structures.

Listing of all publications and technical reports supported under this grant or contract.

None to Date

List of all participating scientific personnel

Name	Position during Program	Times working on Program	Current Status
Brian Cobb	Graduate Student	08/01/07 – 12/31/07	Graduate Student at UT-Austin; no longer on program

Bibliography

- [1] C. G. V. d. Walle, "Band Lineups and Deformation Potentials in the Model-Solid Theory," *Physical Review B*, vol. 39, pp. 1871-1883, 1989.